Elemental Distributions Between Spinel and Liquid Phases in Vanadium-Bearing Slags at High Temperatures

LIAN CHEN, MAO CHEN, YONGQI SUN, and XIAODONG MA

Herein the elemental distributions (V_2O_3, Cr_2O_3, Al_2O_3, and MgO) between spinel and liquid phases were identified in vanadium-bearing slags at 1200 °C to 1600 °C. The methodology includes melting, quenching and EPMA. We found upon increasing temperatures, V_2O_3 concentration in spinel decreased while that in liquid phase increased; and more CaO induced the transfer of V_2O_3 from spinel to liquid phase. This study provided important clues to target adjust elemental distributions among key phases in vanadium-bearing slags.

https://doi.org/10.1007/s11663-023-02807-3

VANADIUM-BEARING products, such as V_2O_5, V_2O_3, Ti–Al–V and Fe–V alloys, VN, *etc*., are widely used in metallurgy, energy materials, chemical engineering, and aerospace industries because of their extreme properties.[1,2] Currently, vanadium-bearing slags, stone coal, steel slags, and spent catalysts account for the main resources for vanadium extraction.[1–4] Among those vanadium resources, vanadium-bearing slags contribute to more than 40 pct of global vanadium outputs,[5] which are discharged as a secondary resource during the utilization of vanadium–titanium magnetite ores for the production of crude steel.

The treatment of vanadium–titanium magnetite ores generally follows several key steps. First, through mineral separation, the vanadium–titanium magnetite ore is enriched into iron concentrates, with the discharge of iron tailings. Second, in a blast furnace, the iron concentrates, after sintering, are smelted and reduced into vanadium-bearing liquid iron, with the discharge of blast furnace slags. Third, in a LD converter, the vanadium in liquid iron is further oxidized into vanadium converting slags (or vanadium-bearing slags), and meanwhile, semi-steel is produced for further steelmaking. Consequently, the high temperature vanadium-bearing slags will be cooled and ground into powders, and after that, the samples will be roasted in the addition of Ca or Na resources under an oxidization atmosphere. After roasting, the samples will be ground, leached and treated through several post-steps, and finally, V_2O_5 will be synthesized as the main product for further utilizations.[6,7]

For the foregoing process, most researches have been performed on the characteristics of roasting and leaching steps. For instance, regarding the roasting step, the effects of roasting agents, Ca resource, Na resource and $(NH_4)_2SO_4$, *etc*., have been systemically investigated as well as roasting temperature and holding time.[8–13] As for the leaching step, the effects of pH, leaching time and acid types have been identified.[14–19] In those researches, a recovery ratio of vanadium from slags is generally employed as a simple parameter to estimate whether the whole process is efficient and feasible. However, the elemental evolutions during the initial cooling process of vanadium-bearing slags, and the chemical compositions of inside phases before roasting have been rarely considered; instead, they are taken as a constant initial state of the slags for further roasting and leaching.

From a very fundamental respect, the original phases and their chemical compositions in cooled vanadium-bearing slags are directly related to the efficiencies of further roasting and leaching, which are determined by the initial chemical compositions and the cooling processes. However, related researches on this topic are almost none. Therefore, the present study was motivated. The elemental distributions among the main phases in vanadium-bearing slags were identified during the cooling process especially at high temperatures.

LIAN CHEN and MAO CHEN are with the Pangang Group Panzhihua Steel Research Institute Co., Ltd. (PANYAN), Panzhihua 617000, P.R. China and also with the State Key Laboratory of Vanadium and Titanium Resources Comprehensive Utilization, Panzhihua 617000, P.R. China. YONGQI SUN is with the School of Metallurgy and Environment and National Center for International Cooperation of Clean Metallurgy, Central South University, Changsha 410083, P.R. China. Contact e-mail: yongqi.sun@csu.edu.cn XIAODONG MA is with the Sustainable Minerals Institute, University of Queensland, Brisbane 4072, Australia.

Manuscript submitted February 3, 2023; accepted April 22, 2023.
Article published online May 1, 2023.

We firstly analyzed an industrial sample collected from PANYAN Company using electron probe X-ray microanalysis (EPMA), and found that the main phases in the cooled vanadium converting slags were spinel, liquid, olivine and residual iron phases, as shown in Figure 1(a). The chemical compositions of those phases are shown in Table I, indicating V_2O_3 was mainly distributed in the spinel and liquid phases. They were two dominant phases in vanadium-bearing slags at high temperatures from the thermodynamic respect, where the spinel phase acted as a primary phase due to its high melting point. Therefore, the clarification of elemental distributions especially V_2O_3 in those two phases is quite significant, since it directly determines the further roasting and leaching efficiencies.

Based on the results of industrial sample, we designed two types of materials, namely base slags with low CaO content (1.8 wt pct), and a sample with high CaO content (18.5 wt pct), as shown in Table II. High purity materials including MgO (99.95 wt pct, Alfa Aesar), MnO (99.99 wt pct, Alfa Aesar), Al_2O_3 (99.5 wt pct, Sigma-Aldrich), SiO_2 (99.9 wt pct, Alfa Aesar), V_2O_3 (99.99 wt pct, Sigma-Aldrich) and Cr_2O_3 (99 wt pct, Alfa Aesar) were used to prepare the samples based on the chemical designs. MgO was heated at 400 °C for 12 hours to remove the moisture. CaO was obtained by the calcination of $CaCO_3$ (99.0 wt pct, Sigma-Aldrich) under an air atmosphere at 950 °C for 16 hours. Regarding the "FeO" in the slags, powder Fe (99.85 wt pct, Goodfellow Cambridge Ltd) and Fe_2O_3 (99. 5 wt pct, Alfa Aesar) were reacted by a mole ratio of 1:1. These powders were first mixed thoroughly, and then pelletized into pellets (~ 0.3 g) for further high temperature experiments.

For high temperature tests, a vertical reaction tube (impervious recrystallized alumina with 30 mm inner diameter) furnace was used, with the $LaCrO_4$ heating elements, as detailed in the previous studies.[20–22] The hot zone, an area with a stable temperature, was determined by a working thermocouple (Pt-30 pct Rh/Pt-6 pct Rh thermocouple), further corrected by a standard thermocouple. The reaction temperature could be thus accurately controlled within 3 °C. Regarding the atmosphere, an ultrahigh purity (99.999 pct) argon gas, with a flow rate of 450 ml/min, was utilized to confirm the experimental conditions especially process partial pressure of oxygen–PO_2 consistent. Regarding the holding time, one hour was used at high temperatures of 1500 °C to 1600 °C, while two hours at medium temperatures of 1200 °C to 1400 °C to ensure an equilibrium.[20–22] Another key factor controlled was the crucible type since the temperatures covered a wide range. At low temperatures of 1200 °C to 1400 °C, an Fe crucible was used to reduce process costs, while at 1450 °C to 1600 °C, a Pt crucible was used.

After high temperature experiments, the samples were quenched, dried, mounted, polished and carbon coated. After those steps, the microstructures and chemical compositions of various phases were measured using a JXA 8200 Electron Probe X-ray microanalyser (EPMA, Japan Electron Optics Ltd, Japan) with Wavelength Dispersive Detectors (WDD). An accelerating voltage of 15 kV and a current of 1.5×10^{-8} A were applied for composition measurements, while a current of 2×10^{-9} A for microstructural observations. Six standards, with accurately confirmed chemical compositions, were utilized as references: $CaSiO_3$ for Ca and Si, $MgAl_2O_4$ for Mg and Al, Fe_2O_3 for Fe, Cr metal for Cr, V metal for V, and Mn metal for Mn (Charles M. Taylor Co., Stanford, California, USA). An ZAF (atomic number effects, absorption and fluorescence) module was used for composition corrections. Additionally, for data collections and treatment in this study, the multivalent oxides such as iron oxides (including FeO and Fe_2O_3), vanadium oxides, chromium oxides, manganese oxides and titanium oxides, in the liquid and spinel phases were recalculated and simplified as "FeO", V_2O_3, Cr_2O_3, MnO, and TiO_2 for the purposes of presentation and comparison.

For the base slags, the microstructures of the inside phases are firstly measured, as shown in Figure 1(b). As noted, two main phases co-existed, namely a spinel and a liquid phase, while the spinel phase acted as a primary phase precipitated. This agreed with the industrial

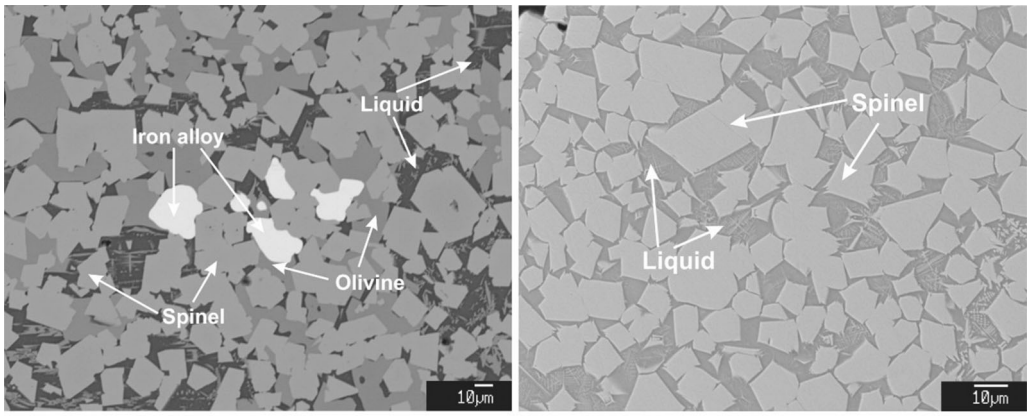

Fig. 1—Microstructures of multiple phases in the vanadium-bearing slags: (*a*) an industrial sample, and (*b*) the base slags.

Table I. Chemical Compositions of the Phases in an Industrial Sample (Weight Percent)

Phase	CaO	MgO	MnO	FeO	SiO_2	TiO_2	V_2O_3	Al_2O_3	Cr_2O_3
Spinel	0.1	2.0	4.0	34.6	0.1	11.9	15.9	4.9	26.6
Olivine	0.3	9.4	9.2	47.6	32.1	0.6	0.4	0.1	0.6
Liquid	9.6	0.6	2.6	11.8	59.0	2.5	0.3	13.2	0.4
Phase	Ca	Mg	Mn	Fe	Si	Ti	V	Al	Cr
Alloy	0.0	0.0	0.1	99.9	0.0	0.0	0.0	0.0	0.0

Table II. Experimental Design of the Samples in this Study

No.	T/°C	CaO	MgO	MnO	FeO	SiO_2	V_2O_3	Al_2O_3	Cr_2O_3
B-1	1200	1.8	2.7	6.4	49.3	14.6	10.5	3.7	11
B-2	1300	1.8	2.7	6.4	49.3	14.6	10.5	3.7	11
B-3	1400	1.8	2.7	6.4	49.3	14.6	10.5	3.7	11
B-4	1450	1.8	2.7	6.4	49.3	14.6	10.5	3.7	11
B-5	1500	1.8	2.7	6.4	49.3	14.6	10.5	3.7	11
B-6	1600	1.8	2.7	6.4	49.3	14.6	10.5	3.7	11
C-1	1200	18.5	2.3	5.3	40.8	12.1	7.5	3	10.6
C-2	1300	18.5	2.3	5.3	40.8	12.1	7.5	3	10.6
C-3	1400	18.5	2.3	5.3	40.8	12.1	7.5	3	10.6
C-4	1500	18.5	2.3	5.3	40.8	12.1	7.5	3	10.6
C-5	1600	18.5	2.3	5.3	40.8	12.1	7.5	3	10.6

sample. Next, the chemical compositions of those phases were measured. We found CaO and SiO_2 mainly occurred in the liquid phase in the whole temperature range. Comparatively, "FeO" acted as a major component in both spinel and liquid phases. We thus mainly discussed the major oxides including V_2O_3 and Cr_2O_3, and the minor oxides including MgO and Al_2O_3, in next sections. Figure 2(a) shows that with increasing temperature, the V_2O_3 concentration in the spinel phase firstly kept stable (~ 24 wt pct, < 1400 °C), and then greatly decreased from ~ 24 wt pct at 1400 °C, to ~ 11 wt pct at 1450 °C, and further to ~ 6 wt pct at 1600 °C. However, the V_2O_3 concentration in the liquid phase had an opposite trend, *i.e.,* it firstly kept a low level (< 1 wt pct) at temperatures below 1400 °C, and then greatly increased from ~ 3 wt pct at 1400 °C, to ~ 9 wt pct at 1450 °C, and further to ~ 12 wt pct at 1600 °C.

Comparatively, the Cr_2O_3 concentrations in spinel and liquid phases were quite different, as shown in Figure 2(b). The Cr_2O_3 concentration in the spinel phase gradually increased with increasing temperature from ~ 25 wt pct at 1200 °C to ~ 40 wt pct at 1600 °C, due to a high melting point of Cr_2O_3 (around 2440 °C) and a strong Cr–O bonding.[23] In other words, Cr_2O_3 worked as a main component of the spinel phase. With increasing temperature, compared to Cr_2O_3, other oxides tended to move from the spinel to the liquid phase, and therefore, a higher Cr_2O_3 concentration in the spinel phase was caused. On the contrary, the Cr_2O_3 concentration in the liquid phase always kept at a low level (< 3 wt pct) and slightly increased from ~ 1 wt pct at 1200 °C to ~ 2 wt pct at 1600 °C.

Regarding the minor MgO, Figure 2(c) shows that its concentration in the spinel phase gradually increased with increasing temperature, *i.e.,* from ~ 1 wt pct at 1200 °C to ~ 3 wt pct at 1600 °C; while that in the liquid phase firstly considerably decreased, *i.e.,* from ~ 9 wt pct at 1200 °C to ~ 3 wt pct at 1300 °C, and then kept relatively stable (~ 3 wt pct) at 1300–1600 °C. Similar to Cr_2O_3, those results could originate from a high melting point of MgO (around 2850 °C).[23,24] However, there was a big difference between MgO and Cr_2O_3, *i.e.,* a high content of MgO remained in the liquid phase even at 1600 °C, because MgO acts as a network modifier in the liquid phase with a strong basicity.[23,24] Opposite to MgO, Figure 2(d) shows that the Al_2O_3 concentration in the spinel phase gradually decreased with increasing temperature, *i.e.,* from ~ 6 wt pct at 1200 °C to ~ 4 wt pct at 1600 °C; while that in the liquid phase increased, *i.e.,* from ~ 0.1 wt pct at 1200 °C to ~ 4 wt pct at 1600 °C. This proved that with increasing temperature, Al_2O_3 moved from the spinel to the liquid phase. From a charge balance respect, Al_2O_3 occupies similar lattice sites to Cr_2O_3 in the spinel phase and a competitive effect between Al_2O_3 and Cr_2O_3 could cause a decreased Al_2O_3 concentration in the spinel phase from the liquid phase upon increasing holding temperature.

For the high CaO content slags, same microstructures as the base slags were detected, *i.e.,* two phases co-existed including a spinel phase and a liquid phase, as not detailed here. The chemical compositions of various phases were then measured, and we found for the major oxides of CaO and SiO_2, they were mainly distributed in the liquid phase, and moreover, their concentration gradually decreased with increasing temperature because more oxides moved from the spinel to the liquid phase, resulting an increasing amount of the liquid phase. As for the "FeO", it was distributed both

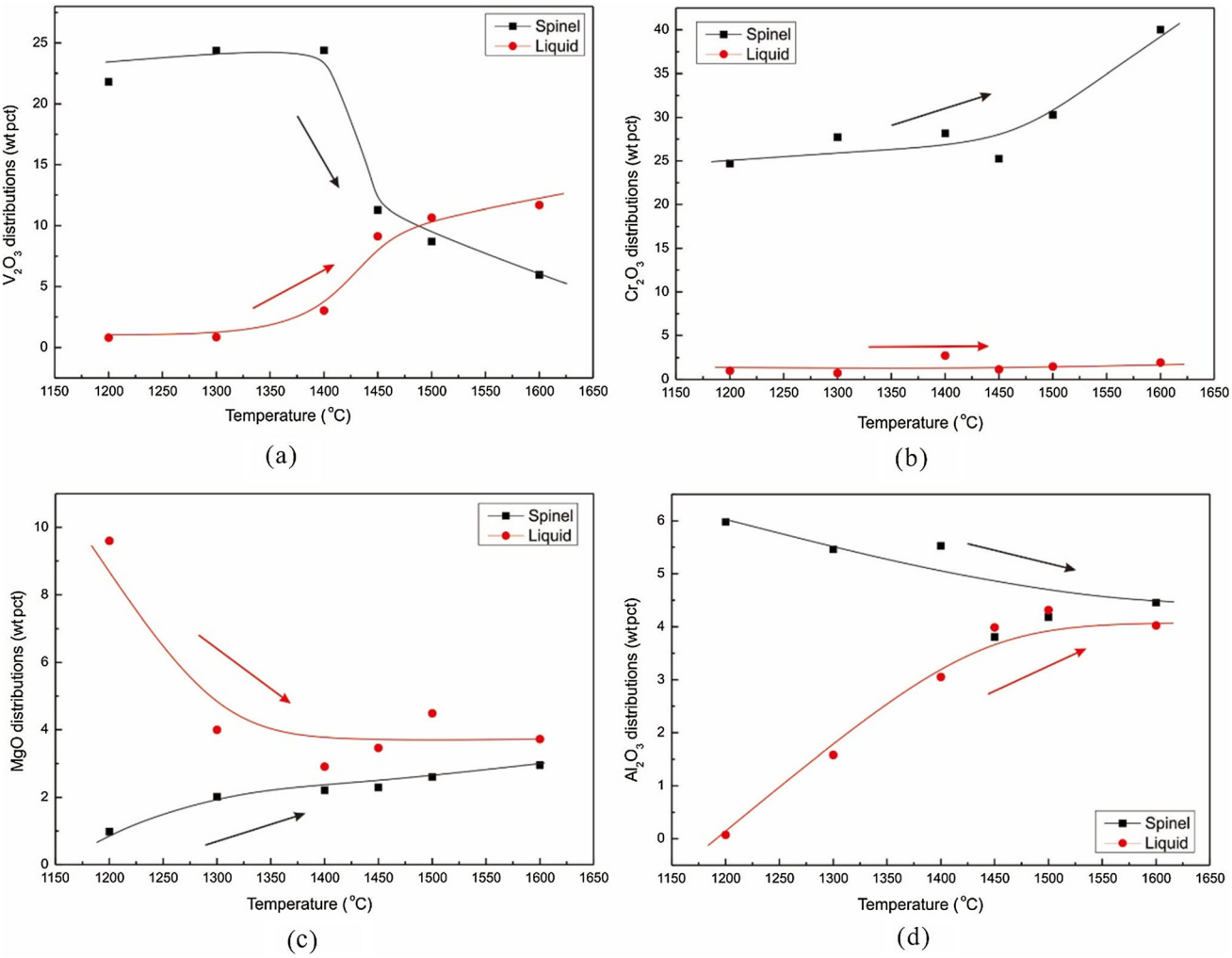

Fig. 2—Elemental distributions between spinel and liquid phases with varying temperature in the base slags: (*a*) V_2O_3, (*b*) Cr_2O_3, (*c*) MgO, and (*d*) Al_2O_3.

in the liquid and the spinel phases while there was not an apparent variation trend among the distributions, similar to the base slags.

Regarding the major oxides of V_2O_3 and Cr_2O_3, they show more clear variation trends between the distributions in spinel and liquid phases, as detailed in Figures 3(a) and (b). With increasing temperature, the V_2O_3 concentration in the spinel phase firstly kept stable (~ 14 wt pct) in the temperature range of 1200 °C to 1400 °C, and then greatly decreased to ~ 1 wt pct at temperature over 1400 °C. On the contrary, the V_2O_3 concentration in the liquid phase greatly increased with increasing temperature, from less than 1 wt pct at 1200 °C to ~ 12 wt pct at 1500 °C to 1600 °C. Comparatively, Cr_2O_3 was mainly present in the spinel phase in the whole temperature range due to its high melting point, which actually determined the primary phase of this slag system. As the temperature increased, the Cr_2O_3 concentration in the spinel phase slightly increased, agreeing with those in the base slags.

As for the minor oxide of MgO, Figure 3(c) shows that its concentration in the spinel phase continuously increased with increasing temperature, *i.e.,* from ~ 2 wt pct at 1200 °C to ~ 5 wt pct at 1600 °C, because of its high melting point. Comparatively, the MgO concentration in the liquid phase remained stable at high temperature of 1400 °C to 1600 °C (~ 2 wt pct). As noted from Figure 3(d), the Al_2O_3 concentration in the spinel phase slightly decreased with increasing temperature, *i.e.,* from ~ 5 wt pct at 1200 °C to ~ 4 wt pct at 1600 °C. However, the variation of Al_2O_3 concentration in the liquid phase was not continuous although an overall decreasing variation with increasing temperature could be observed.

Based on the results of base slags and high CaO content slags, the role of CaO on the elemental distributions between spinel and liquid phases could be clarified. Comparison of Figures 2(a) and 3(a) indicates that an increasing CaO content would induce a higher V_2O_3 concentration in the liquid phase, with a lower V_2O_3 concentration in the spinel phase. This was caused by a strong acidic-basic bonding between CaO and V_2O_3, *i.e.,* in the present system, V_2O_3 mainly acted as a network former, opposite to CaO, a strong network

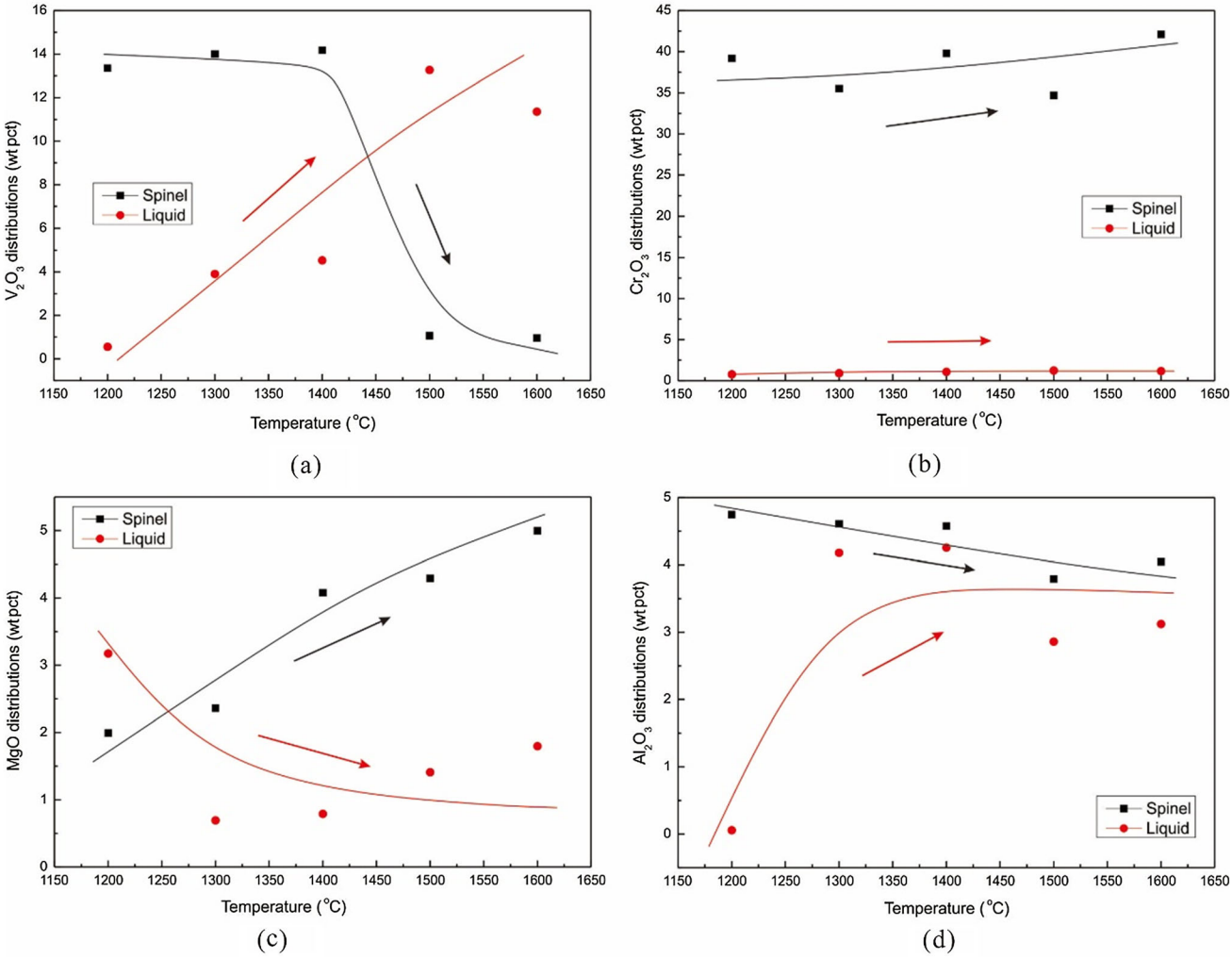

Fig. 3—Elemental distributions between spinel and liquid phases with varying temperature in the high CaO content slags: (*a*) V_2O_3, (*b*) Cr_2O_3, (*c*) MgO, and (*d*) Al_2O_3.

modifier. However, there was a relatively high concentration of V_2O_3 content in the spinel phase of base slags in the whole temperature range, which originated from its high melting point (around 2050 °C).[23] On the other hand, MgO and Cr_2O_3 mainly determined the primary phase of this slag system, namely spinel, due to their high melting points and lattice roles.

Based on the comparison of Figures 2(b) and (d) and 3(b) and (d), the roles of CaO on Cr_2O_3 and Al_2O_3 distributions could be further analyzed. With increasing CaO content, the Cr_2O_3 concentration in the spinel phase remarkably increased. CaO was mainly present in the liquid phase, which could bond more V_2O_3 and Al_2O_3 in the liquid phase, two main components of the spinel phase. Therefore, the relative concentrations of V_2O_3 and Al_2O_3 in the spinel phase decreased, and that of Cr_2O_3 increased. In consistence, the relative concentration of Cr_2O_3 in the liquid phase slightly decreased with the increasing CaO content. In comparison, Figures 2(c) and 3(c) show that the influence of CaO on the MgO distributions was quite different. With high content of CaO, MgO concentration in the spinel phase remarkably increased while that in the liquid phase decreased. From a respect of network roles in the structures, CaO and MgO both act as network modifiers with CaO having a stronger network modifying ability.[23,24] CaO would replace the local sites of MgO in the liquid networks, and therefore, a higher CaO content would induce a decreased MgO concentration in the liquid phase by this replacement effect, and correspondingly, an increased MgO concentration would occur in the spinel phase.

According to the foregoing analyses, the clues to adjust the elemental distributions especially V_2O_3 between the spinel and liquid phases could be clarified. The first strategy was based on the role of CaO. An increasing CaO content would enhance the transfer of V_2O_3 from the spinel to the liquid phase due to their different network roles and strong bonding. The varying distribution of V_2O_3 would not only affect the converting process such as the overall recovery rate of vanadium from the liquid iron to the slags but also affect the

further roasting process since the kinetics between the spinel and liquid phases with the roasting materials such as NaOH, $CaCO_3$ and $(NH_4)_2SO_4$ could be quite different.[8–13]

The second strategy was based on the elemental distributions with varying temperatures. An increasing temperature would induce an increasing V_2O_3 concentration in the liquid phase. Therefore, before cooling process, holding the slags at a higher temperature for a longer period would enhance the distribution of V_2O_3 in the liquid instead of the spinel phase. Another method followed a similar principle, controlling the cooling rate. Upon rapidly cooling, the slags after cooling would be much closer to the state at high temperatures since the phases at high temperatures remained to a larger extent. However, upon slowly cooling, the slags would be closer to the state at low temperatures since the phases could fully evolve. As a result, to rapidly cool the slags would increase the V_2O_3 concentration in the liquid phase from the spinel phase, further improving the roasting and leaching efficiencies.

In summary, we investigated the elemental distributions between spinel and liquid phases upon cooling of vanadium-bearing slags, where both the major oxides of CaO, SiO_2, FeO, V_2O_3 and Cr_2O_3 and the minor oxides of MgO and Al_2O_3 were considered. The results show that an increasing temperature decreased the V_2O_3 and Al_2O_3 concentrations in the spinel phase, while the Cr_2O_3 and MgO concentrations increased, *i.e.,* the latter two oxides determined the primary phase of the vanadium-bearing slags. We further found that a higher content of CaO enhanced the movement of V_2O_3 from the spinel to the liquid phase due to the strong bonding of CaO–V_2O_3. Our study thus provided important clues to modify the elemental distributions among key phases in vanadium-bearing slags at high temperatures.

ACKNOWLEDGMENTS

The authors thank the PANYAN-UQ Collaborative Research Project (2019001288), The National Science Fund for Overseas Excellent Young Scholars (21FAA01748) and the National Natural Science Foundation of China (52274415) for financial support. The authors acknowledge the facilities and the scientific and technical assistance of the Australian Microscopy & Microanalysis Research Facility, Centre for Microscopy and Microanalysis, The University of Queensland.

CONFLICT OF INTEREST

On behalf of all authors, the corresponding author state that there is no conflict of interest.

REFERENCES

1. R.R. Moskalyk and A.M. Alfantazi: *Miner. Eng.*, 2003, vol. 16, pp. 793–805.
2. B. Voglauer, A. Grausam, and H.P. Jörgl: *Miner. Eng.*, 2004, vol. 17, pp. 317–21.
3. H. Fang, H. Li, T. Zhang, B. Liu, and B. Xie: *ISIJ Int.*, 2015, vol. 55, pp. 200–06.
4. K. Hu, X. Liu, and Q. Li: *Metall. Mater. Trans. B*, 2017, vol. 48B, pp. 1342–347.
5. J. Zhang, W. Zhang, L. Zhang, and S. Gu: *Int. J. Miner. Process.*, 2015, vol. 138, pp. 20–9.
6. Y. Wu, G. Zhang, and K.C. Chou: *Metall. Mater. Trans. B*, 2016, vol. 47B, pp. 3405–412.
7. Y. Wu, G. Zhang, and K.C. Chou: *Metall. Mater. Trans. B*, 2018, vol. 49B, pp. 3570–579.
8. J. Wen, T. Jiang, Y. Xu, J. Liu, and X. Xue: *Metall. Mater. Trans. B*, 2018, vol. 49B, pp. 1471–481.
9. Y. Ji, S. Shen, J. Liu, and Y. Xue: *J. Clean. Prod.*, 2017, vol. 149, pp. 1068–078.
10. X. Li, B. Xie, G. Wang, and X. Li: *Trans. Nonferrous Met. Soc. China*, 2011, vol. 21, pp. 1860–867.
11. G. Zhang, D. Luo, C. Deng, L. Lv, B. Liang, and C. Li: *J. Alloys Compd.*, 2018, vol. 742, pp. 504–11.
12. L. Liu, Z. Wang, H. Du, S. Zheng, U. Lassi, and Y. Zhang: *Int. J. Miner. Process.*, 2017, vol. 160, pp. 1–7.
13. Z. Wang, S. Zheng, S. Wang, Y. Qin, H. Du, and Y. Zhang: *Hydrometallurgy*, 2015, vol. 151, pp. 51–5.
14. H. Li, K. Wang, W. Hua, Z. Yang, W. Zhou, and B. Xie: *Hydrometallurgy*, 2016, vol. 160, pp. 18–25.
15. H. Li, H. Fang, K. Wang, W. Zhou, Z. Yang, X. Yan, W. Ge, Q. Li, and B. Xie: *Hydrometallurgy*, 2015, vol. 156, pp. 124–35.
16. Z. Yang, H. Li, X. Yin, Z. Yan, X. Yan, and B. Xie: *Int. J. Miner. Process.*, 2014, vol. 133, pp. 105–11.
17. J. Xiang, Q. Huang, X. Lv, and C. Bai: *J. Clean. Prod.*, 2018, vol. 170, pp. 1089–101.
18. J. Xiang, Q. Huang, X. Lv, and C. Bai: *J. Hazard. Mater.*, 2017, vol. 336, pp. 1–7.
19. J. Zhang, W. Zhang, L. Zhang, and W. Gu: *Solvent Extr. Ion Exch.*, 2014, vol. 32, pp. 221–48.
20. Y. Sun, M. Chen, Z. Cui, L. Contreras, and B. Zhao: *Metall. Mater. Trans. B*, 2020, vol. 51B, pp. 426–32.
21. Y. Sun, M. Chen, Z. Cui, L. Contreras, and B. Zhao: *Metall. Mater. Trans. B*, 2020, vol. 51B, pp. 1–5.
22. M. Chen, Y. Sun, E. Balladares, C. Pizarro, and B. Zhao: *Calphad*, 2019, vol. 66, p. 101642.
23. Y. Waseda and J.M. Toguri: *The Structure and Properties of Oxide Melts: Application of Basic Science to Metallurgical Processing*, World Scientific, Singapore, 1998.
24. Y. Sun, M. Chen, and B. Zhao: *J. Non-Cryst. Solids*, 2019, vol. 515, pp. 50–7.